ISSN 1063-7834, Physics of the Solid State, 2022, Vol. 64, No. 4, pp. 204–209. © Pleiades Publishing, Ltd., 2022.
ISSN 1063-7834, Physics of the Solid State, 2022. © Pleiades Publishing, Ltd., 2022.
Russian Text © The Author(s), 2022, published in Fizika Tverdogo Tela, 2022, Vol. 64, No. 8, pp. 920–926.

Microstructure and Physical and Mechanical Properties of the $Al_{90}Gd_{10}$ Binary Alloy after Barothermal Treatment

S. G. Menshikova[a], *, A. A. Shushkov[a], and V. V. Brazhkin[b]

[a] *Udmurt Federal Research Center, Ural Branch, Russian Academy of Sciences, Izhevsk, Russia*
[b] *Institute for High Pressure Physics, Russian Academy of Sciences, Troitsk, Moscow, Russia*
**e-mail: svetlmensh@mail.ru*

Received April 25, 2022; revised April 25, 2022; accepted April 26, 2022

Abstract—Using the microindentation, X-ray diffraction, optical microscopy, and electron microscopy methods, the microstructure and bulk physical and mechanical properties (hardness, reduced elastic modulus, plasticity index, elastic recovery parameter) of two samples of the $Al_{90}Gd_{10}$ binary hypereutectic alloy (hereinafter, formula indices correspond to at %) are studied. The first sample is obtained by rapid cooling of the melt at a rate of 1000 degree/s at a high pressure of 10 GPa; the hardening temperature is 1800 K. The second sample is obtained by pressing the original sample with a high pressure of 5 GPa without melting. Compared to the intial sample, the microstructure of both samples is crushed and compacted. The structure of the initial sample is comprised of two equilibrium phases of α-Al and Al_3Gd. In the sample prepared without melting, a phase with composition $Gd_{55}Al_{45}$ is found in addition to the α-Al and Al_3Gd phases; in the sample prepared with melting, a phase with composition $Al_{92}Gd_8$ is found. Features of the structure morphology and changes in the phase composition of the samples prepared under high pressure lead to changes in the physical and mechanical properties of the studied alloy.

Keywords: high pressure, melt, phase, microstructure, physical and mechanical properties, indentation
DOI: 10.1134/S1063783422050055

1. INTRODUCTION

Rare earth metals (REMs) are successfully used as alloying additives to alloys and substantially improve the performance properties of the latter, including the improvement of performance at elevated temperatures, as well as contribute to grain refinement and increase the corrosion resistance of alloys. The Al–REM alloys have high structural properties and can serve in the future as highly resistive and energy saving components. Materials in amorphous and amorphous nanocrystalline states are obtained with REM concentrations of less than 20% [1]. Recently, the structure and properties of alloys of these systems have been actively studied.

The Al–Gd system, like most Al–REM systems, has a phase diagram with the eutectic point. In the solid state, the existence of the following five stable chemical compounds has been established: Al_3Gd, Al_2Gd, AlGd, Al_2Gd_3, and $AlGd_2$ [2]. The authors of [3] also report the presence of the Al_4Gd compound in the system. In [4], the $Al_{17}Gd_2$ compound is reported. All alloys of the Al–Gd system obtained under equilibrium conditions consist of the two stable phases in the region rich in aluminum: α-Al and Al_3Gd. The eutectic point corresponds to 2% Gd. The solubility of Gd in Al is practically absent.

According to [5], liquid Al–Gd alloys are microheterogeneous in the range of low Gd contents; with little overheating above the liquidus, the groups with the arrangement of atoms close to the arrangement of atoms in the Al_3Gd intermetallic compound are retained. These groups are destroyed upon heating. The authors of [6] also report the formation of the microgroups of atoms in melts, which are ordered according to the Al_2Gd type and remain in the melt even with high overheating relative to the liquidus up to 2000 K. According to [7], the structure of melts consists of a disordered region containing randomly arranged groups of the type of compound Al_xREM_y. With an increase in the REM content, the interaction of different sorts of atoms predominates, which leads to the formation of stable complexes.

It is known that the state of the melt before quenching has an effect on the structure and properties of alloys [8]. Various extreme effects, in particular, high pressure (several gigapascals) exert an influence on the thermodynamics and solidification kinetics of the melt and lead to various changes in the structure of the alloys [9]. The progress made in understanding the structure formation processes occurring in glass-

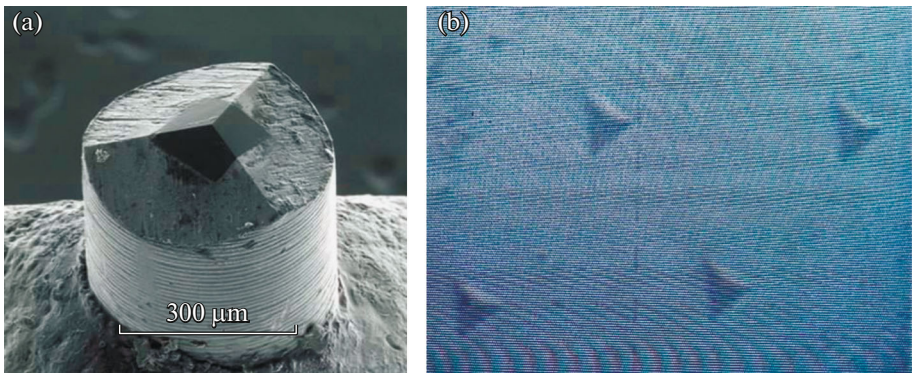

Fig. 1. (a) Berkovich indenter; (b) imprints.

forming melts in the eutectic region, as well as in studying the effect of the pressure and cooling rate on solidification processes, is of high scientific significance and relevance. It is known that many compounds are readily synthesized under high pressure, and a number of them cannot be obtained at all without the use of high pressure technology. In this case, new structures (crystals, glasses, and gels) and new phases with new unique properties that are impossible in the absence of external influences are formed. The mechanism of action of high pressures and temperatures on the structure and properties of alloys is different in different systems [10–14].

In the chosen Al–Gd model system, the influence of high pressure on the kinetics of formation of both stable and metastable phases was expected. The purpose of this study was aimed at investigating the microstructure, phase composition, and physical and mechanical properties of the $Al_{90}Gd_{10}$ alloy prepared by barothermal treatment.

2. MATERIALS AND TECHNIQUES

An ingot with composition $Al_{90}Gd_{10}$ was prepared by melting the metals in corundum crucibles in a Tamman furnace. The initial components were elements with the following contents of the base metal: 99.999 wt % in aluminum and 99.9 wt % in gadolinium. The chemical analysis of the ingot showed that the content of the main components corresponded to the specified composition within ±0.25% of the nominal value. The resulting ingot was considered as an initial sample.

Samples for research were obtained in a toroidal high pressure chamber [15]. The first sample was obtained by rapid cooling of the melt at a rate of 1000 deg/s under a high pressure of 10 GPa (sample with melting); the hardening temperature was 1800 K. A solid body (Algeti stone) was used as a pressure transmitting medium. The sample was heated and molten by passing an alternating current through the material placed in a crucible made of hexagonal boron nitride. The temperature value was calculated using the thyristor readings based on the current power. The second sample was obtained by pressing original sample at a high pressure of 5 GPa (sample without melting). The phase composition of the samples was determined by the X-ray diffraction (XRD) method on a Dron-6 setup equipped with a CuK_α radiation source. To determine the chemical structure and elemental composition, and the morphology and size of the structural components of the alloy, a Quattro S scanning electron microscope (SEM) equipped with a standard DBS (directional backscatter) detector of the ABS/CBS system was used. The error in determining the percentage of elements in the samples was no more than 5%.

The measurements and calculation of the physical and mechanical characteristics of the samples under study were carried out on a Nanotest 600 integrated measurement system using a Berkovich indenter (a trihedral diamond pyramid with an apex angle of 65.3° and a curvature radius of about 200 nm) (Fig. 1).

The H/E_r ratio of the hardness to the reduced elastic modulus was used to assess the degree of material hardening. The H/E_r value characterizes the ability of a material to change its shape and size during deformation, and can also serve as a qualitative relative characteristic of the resistance of materials to deformation under mechanical loading, thereby reflecting its structural state [16]. The hardness and reduced elastic modulus were calculated in accordance with the Oliver–Pharr method [17]. The hardness and reduced elastic modulus were determined by analyzing the unloading curve and the indentation depth on the basis of the loading–unloading diagram obtained during the tests with a diamond indenter. The duration of loading and unloading of the indentation point was 10 s. The maximum force equal 200 mN was applied to the samples, since the properties were measured in the bulk. The delay time under the maximum loading force was 10 s. The distance between the indentation points was 100 μm. For each sample, at least thirty measurements were performed. The elastic recovery

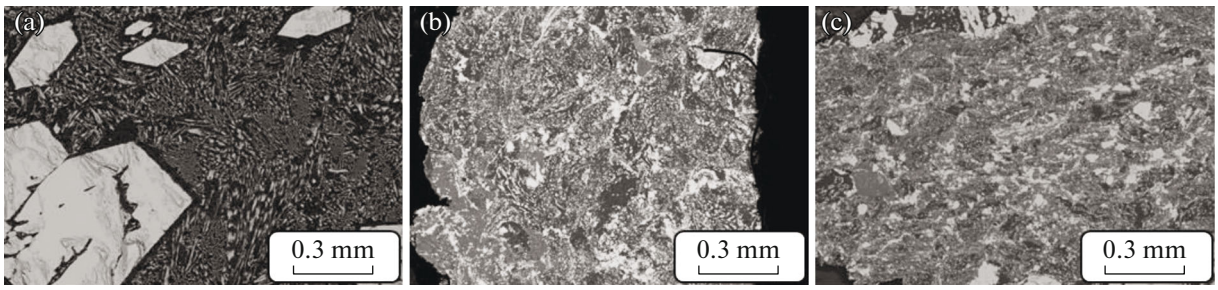

Fig. 2. Microstructure of (a) the initial ingot, (b) the ingot pressed under a high pressure of 5 GPa without melting; and (c) the ingot prepared from a melt under a high pressure of 10 GPa (1800 K, 1000 degree/s).

parameter (ERP) was also calculated as the ratio of the difference between the maximum and plastic depths to the depth of plastic penetration of the diamond indenter. The plasticity index (PI) parameter was calculated as the ratio of the amount of work W_{pl} spent for the formation of plastic strain to total work $W_{tot} = W_{pl} + W_{el}$, where W_{el} is the work spent for the formation of elastic strain.

3. RESULTS AND DISCUSSION

3.1. Microstructure

Figure 2 compares the microstructures of (a) the initial ingot, (b) the ingot pressed under a high pressure of 5 GPa without melting, and (c) the ingot prepared from the melt under a high pressure of 10 GPa (1800 K, 1000 degree/s). According to the XRD data, the structure of the initial ingot is represented by the following two equilibrium phases: α-Al and Al_3Gd (type D0.19, hexagonal hP8/3). Large white primary crystals of the Al_3Gd phase can be clearly seen in Fig. 2a, around which a platelet–rod eutectic (α-Al + Al_3Gd) is formed.

The phase composition of the sample corresponds to the equilibrium phase diagram of the alloy [2]. As can be seen from Fig. 2, the microstructure of the samples obtained under high pressure is more dispersed compared to the initial sample. In addition, other phases beside the α-Al and Al_3Gd phases were found in each sample. In the sample prepared without melting, a phase with composition $Gd_{55}Al_{45}$ in the form of small cuboids formed around large crystals in a small amount (Fig. 3). Table 1 shows its elemental analysis. In the sample prepared with melting, there is a phase with composition $Al_{92}Gd_8$ (Fig. 4). Its elemental analysis is given in Table 2. Figure 5 shows the concentration maps of the distribution of elements in both samples. Thus, the phase compositions of the samples vary.

Table 1. Elemental analysis of the phase enriched in Gd

Element	wt %	at %
Al	12.5	45.0
Gd	87.5	55.0

Table 2. Elemental analysis of the phase enriched in Al

Element	wt %	at %
Al	64.9	92.0
Gd	35.1	8.0

3.2. Physical and Mechanical Properties

Table 3 shows the physical and mechanical characteristics of the samples under study. For samples obtained under high pressure, only averaged values of properties were taken into consideration, given the dispersity of their structure.

Table 3 shows that the average value of hardness H of the initial sample of the $Al_{90}Gd_{10}$ alloy is about 3.5 GPa, as calculated from the data of measurements of hardness H for intermetallic compound Al_3Gd and eutectic (α-Al + Al_3Gd). Figure 6 shows separately the hardness of intermetallic compound Al_3Gd and eutectic (α-Al + Al_3Gd). The main contribution to the hardness value is made by the intermetallic compound, since the hardness value of the intermetallic compound is 7.4 times higher than the hardness value of the eutectic. At the same time, Table 3 shows that plasticity index PI of intermetallic compound Al_3Gd is almost two times lower than plasticity index PI of eutectic (α-Al + Al_3Gd), i.e., the strain is more elastic, which explains the high hardness value of intermetallic compound Al_3Gd. Plasticity indices PI of both samples obtained under high pressure are close to plasticity index PI of eutectic (α-Al + Al_3Gd) formed from the initial sample. Elastic recovery parameter ERP in the sample prepared from the melt is 1.6 times higher than in the sample prepared without melting.

The performed studies have shown that the average value of hardness H in the sample prepared with melt-

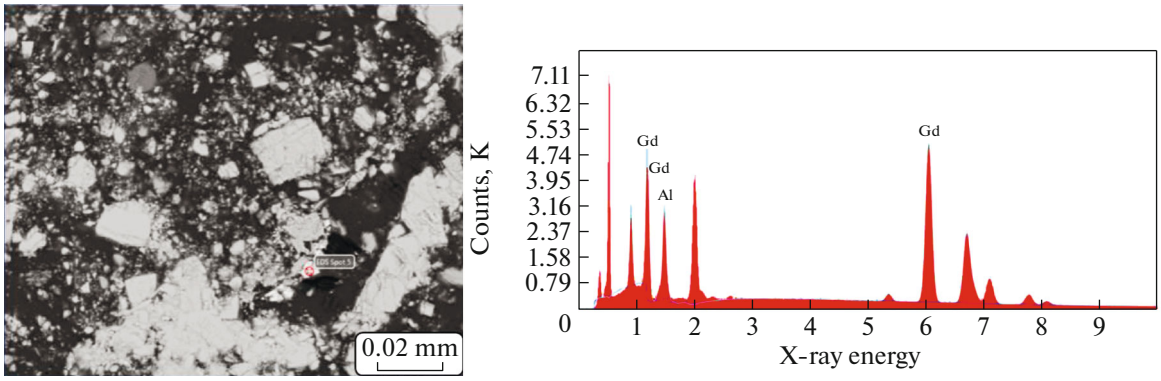

Fig. 3. Data on the X-ray spectral microanalysis of the phase enriched in Gd in the sample prepared by pressing under a high pressure of 5 GPa without melting.

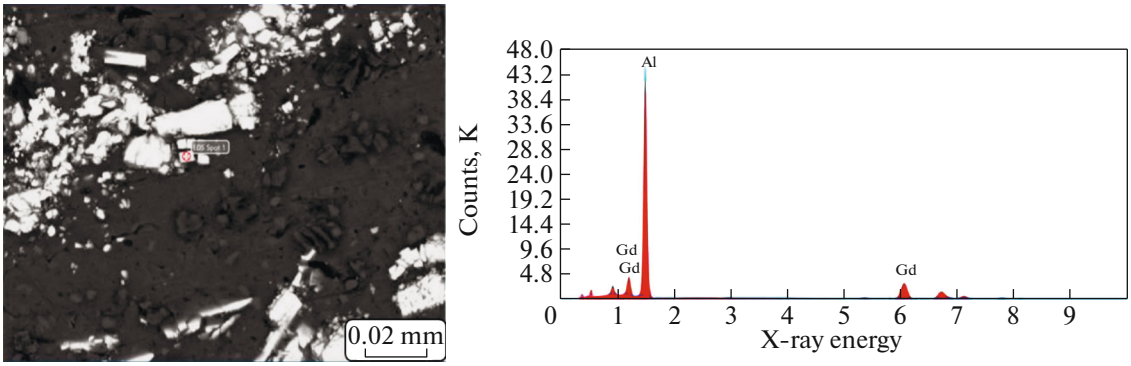

Fig. 4. Data on the X-ray spectral microanalysis of the phase enriched in Al in the sample prepared from a melt under a high pressure of 10 GPa (1800 K, 1000 degree/s).

ing is 1.2 times higher than in the sample prepared by pressing without heating, while the average value of reduced elastic modulus E_r in the former is 1.3 times lower.[1] Moreover, the H/E_r ratio of the degree of hardening in the sample prepared with melting is 1.6 times higher than in the sample prepared by pressing without heating. The consideration of the $Gd_{55}Al_{45}$ phase in the sample without melting leads to increases in the average hardness of the sample by a factor of almost 10 and in the reduced elastic modulus by a factor of 2.4, since the hardness of this phase is about 10 GPa based on the test results. The $Gd_{55}Al_{45}$ phase is poorly observed in the microscope of the Nanotest 600 measurement system and it took a lot of effort to clearly hit into it with a diamond indenter. Figure 7 shows loading–unloading curves for measurements with a hardness of about 10 GPa and, for comparison, nineteen measurement data obtained in other points of the sample. As can be seen from Fig. 7, the maximum penetration depth of the diamond tip for measurement with the obtained hardness value of about 10 GPa is substantially lower (h_{max} = 963.37 nm) compared to

[1] The comparison is carried out without consideration of the detected $Gd_{55}Al_{45}$ phase.

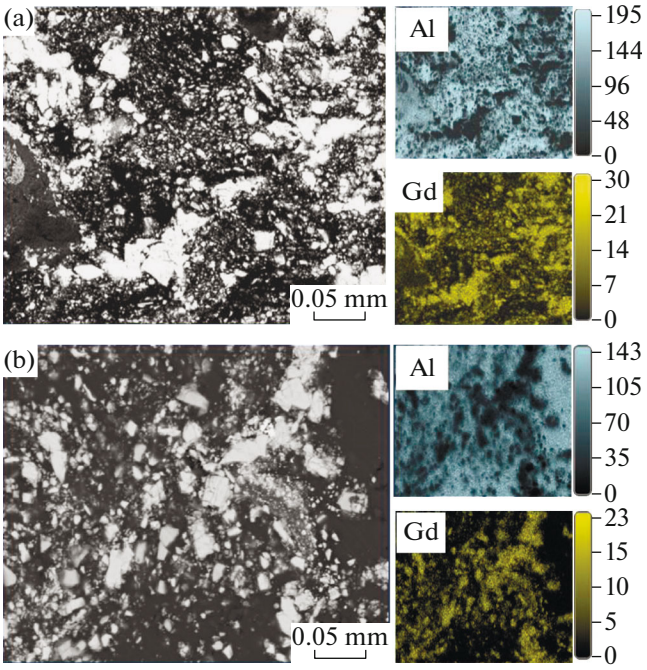

Fig. 5. Concentration maps of the distribution of elements over the sample for the samples prepared (a) with melting and (b) without melting.

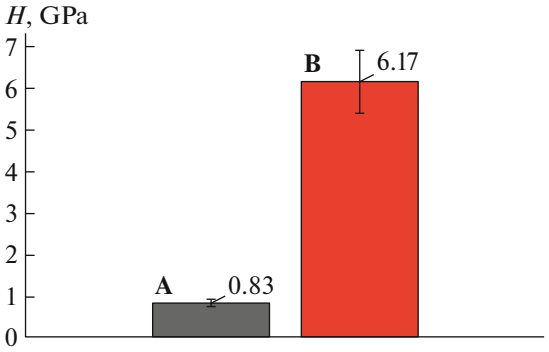

Fig. 6. Hardness values H (GPa) of (**A**) the α-Al + Al_3Gd eutectic mixture and (**B**) intermetallic compound Al_3Gd in the initial sample.

the average value of the maximum depth for nineteen measurement points (h_{max} = 3039.25 nm), which gives rise to a high hardness value. For the sample prepared with melting, it was not possible to hit into the detected $Al_{92}Gd_8$ phase with a diamond indenter.

4. CONCLUSIONS

We have studied the physical and mechanical characteristics of samples obtained under high pressure in comparison with the initial sample. The progress made in understanding the structure formation processes occurring in the eutectic region in glass-forming melts of the Al–REM type (REM stand for rare earth metal), including the $Al_{90}Gd_{10}$ alloy investigated in this study, and in studying the effects of the pressure and cooling rate on the solidification processes is of high scientific and practical significance, since the study of the processes leading to an increase in the strength properties of materials and the hardening mechanisms and the development of effective technologies for the preparation of high-strength materials on this basis are the fundamental problems of modern materials science in instrumentation, which have to be solved. Without these kinds of materials, the further development of mechanical engineering, aviation, space technology, shipbuilding, mining, and nuclear energy is impossible. Under conditions of high pressures and temperatures, the physical and chemical processes are observed during solidification of the melt, which are hindered under normal conditions or impossible due to thermodynamic limitations.

For the $Al_{90}Gd_{10}$ alloy, the performed studies have shown that the impact of high pressure leads to a change in the phase composition, and has effects on the microstructure and the physical and mechanical properties of the alloy. The formation of new phases is detected in the alloy, the study of which requires additional efforts. The samples prepared under pressure have crushed and compacted structures and exhibit high mechanical properties that are determined by dispersion strengthening and grain boundary strengthening. The dispersion strengthening is achieved as a result of precipitation of the detected dispersed phase with high hardness values and reduced elastic modulus under pressure treatment of the alloy. The grain boundary strengthening is caused by the fact that grain boundaries serve as obstacles to the movement of defects such as dislocations. If the stress necessary for the operation of the source of dislocations in a grain with a favorable orientation is reached earlier than in the neighboring grain, then movement occurs first in the favorably oriented grain and then accumu-

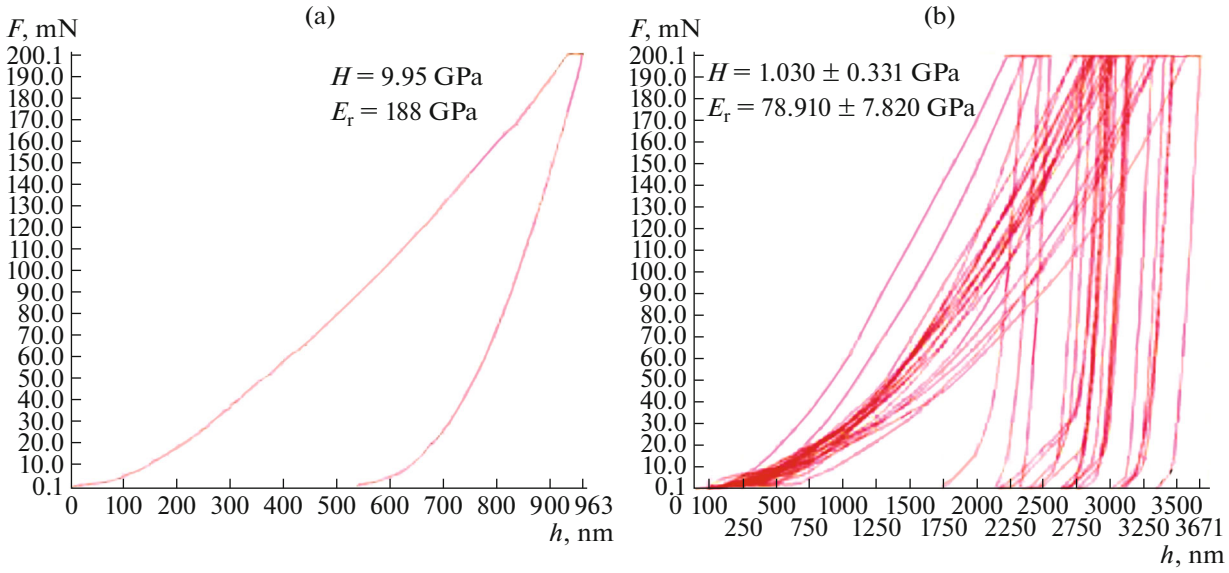

Fig. 7. Dependences of the applied force on the depth of indenter penetration into (a) the $Gd_{55}Al_{45}$ phase and (b) other points of the sample for the sample prepared without melting.

Table 3. Values of the physical and mechanical characteristics of the studied samples

Characteristic	Initial sample (eutectic + intermetallic compound)	Initial sample (eutectic)	Initial sample (intermetallic compound)	Sample without heating	Sample with heating
H, GPa	3.500 ± 2.440	0.830 ± 0.094	6.170 ± 0.750	1.030 ± 0.331	1.270 ± 0.440
E_r, GPa	76.870 ± 8.070	74.230 ± 4.460	84.040 ± 11.380	78.910 ± 7.820	60.440 ± 12.080
H/E_r	0.028 ± 0.029	0.011 ± 0.009	0.073 ± 0.007	0.013 ± 0.003	0.021 ± 0.005
PI	0.800 ± 0.190	0.910 ± 0.009	0.505 ± 0.122	0.890 ± 0.027	0.820 ± 0.040
W_{pl}, nJ	173.480 ± 78.410	218.96 ± 19.501	50.040 ± 12.210	191.440 ± 29.034	168.801 ± 28.350
W_{el}, nJ	28.220 ± 14.211	20.550 ± 1.317	49.030 ± 12.210	22.840 ± 3.680	35.241 ± 6.091
ERP	0.099 ± 0.103	0.037 ± 0.003	0.265 ± 0.266	0.044 ± 0.011	0.072 ± 0.019

lation of dislocations that have approached to the grain boundary. The resulting stress fields are superimposed on the external ones, and this can lead to the fact that the yield stress is reached in neighboring grains. In this way, plastic deformation propagates into neighboring grains. The process becomes more hindered when the grain size decreases (which is observed in our case), the number of dislocations accumulated at the grain boundaries decreases, the stress fields decrease, and most importantly, the set of grain misorientations increases, which generally makes the boundaries a more effective obstacle.

The results obtained in this study once again confirm the effectiveness of the influence of extreme impacts, namely, the combination of high pressures, temperatures, and rapid hardening, on the structure and properties of the synthesized materials.

ACKNOWLEDGMENTS

The authors express their sincere gratitude to V.I. Lad'yanov, Dr. Sci. (Phys.–Math.), and A.V. Vakhrushev, Dr. Sci. (Phys.–Math.), for valuable advices given in the course of study, as well as to I.K. Averkiev for his assistance in performing the elemental analysis of the samples.

FUNDING

This study was supported in part by the Russian Science Foundation (grant no. 22-22-00674). Electron microscopic studies and measurements of physical and mechanical properties were performed using the equipment of Center for Collective Use Center for Physical and Physicochemical Methods of Analysis and for Studying Properties and Characteristics of Surfaces, Nanostructures, Materials and Products at the Udmurt Federal Research Center, Ural Branch, Russian Academy of Sciences (Izhevsk, Russia). Samples under high pressure were prepared in the Institute for High Pressure Physics, Russian Academy of Sciences (Troitsk, Moscow, Russia).

CONFLICT OF INTEREST

The authors declare that they have no conflicts of interest.

REFERENCES

1. I. Inoue, Prog. Mater. Sci. **43**, 365 (1998).
2. *State Diagrams of Binary Metallic Systems,* Ed. by N. P. Lyakishev (Mashinostroenie, Moscow, 1996), Vol. 1 [in Russian].
3. O. J. C. Runnals and R. R. Boucher, J. Less-Common Met. **13**, 431 (1967).
4. I. Pop, N. Dihoiu, M. Coldea, and C. Hagan, J. Less-Common Met. **64**, 63 (1979).
5. S. V. Golubev and V. I. Kononenko, Rasplavy **6**, 100 (1991).
6. V. Sidorov, O. Gornov, V. Bykov, L. Son, R. Ryltsev, S. Uporov, V. Shevchenko, V. Kononenko, K. Shunyaev, N. Ilynykh, G. Moiseev, T. Kulikova, and D. Sordelet, Mater. Sci. Eng. **449**, 586 (2007).
7. S. V. Golubev and V. I. Kononenko, Rasplavy **2**, 35 (1988).
8. I. G. Brodova, P. S. Popel', N. M. Barbin, and N. A. Vatolin, *Melts as the Basis for the Formation of the Structure and Properties of Aluminum Alloys* (Yekaterinburg, UrO RAN, 2005).
9. G. E. Abrosimova and A. S. Aronin, Phys. Solid State **59**, 2248 (2017).
10. S. V. Popova, O. A. Sazanova, V. V. Brazhkin, N. V. Kalyaeva, M. B. Kondrin, and A. G. Lyapin, Phys. Solid State **48**, 2177 (2006).
11. E. V. Dedyaeva, T. K. Akopyan, A. G. Pedalko, G. V. Talanova, G. I. Zabarev, A. D. Izotov, A. N. Suchkov, V. T. Fedotov, and L. I. Shorneva, Inorg. Mater. **52**, 1077 (2016).
12. R. Xu, Mater. Lett. **59**, 2718 (2005).
13. S.-W. He, Liu Yuanqing, and S. Guo, Heat Treatm. Met. **34** (11), 47 (2009).
14. V. O. Esin, A. S. Krivonosova, I. Zh. Sattybaev, T. G. Fedorova, and V. A. Sazonova, Phys. Met. Metallogr. **107**, 588 (2009).
15. V. V. Brazhkin, Doctoral (Phys.-Math.) Dissertation (Moscow, 1996).
16. Yu. A. Khokhlova, D. A. Ishchenko, and M. A. Khokhlov, Tekh. Diagn. Nerazr. Kontrol', No. 1, 30 (2017).
17. W. C. Oliver and G. M. Pharr, J. Mater. Res. **7**, 1564 (1992).

Translated by O. Kadkin